

The 2dF QSO Redshift Survey – IX. A measurement of the luminosity dependence of QSO clustering

Scott M. Croom,^{1*} B. J. Boyle,¹ N. S. Loaring,² L. Miller,² P. J. Outram,³
T. Shanks³ and R. J. Smith⁴

¹Anglo-Australian Observatory, PO Box 296, Epping, NSW 2121, Australia

²Department of Physics, Oxford University, Keble Road, Oxford OX1 3RH

³Physics Department, University of Durham, South Road, Durham DH1 3LE

⁴Astrophysics Research Institute, Liverpool John Moores University, 12 Quays House, Egerton Wharf, Birkenhead CH41 1LD

Accepted 2002 April 29. Received 2002 April 29; in original form 2001 October 2

ABSTRACT

In this paper we present a clustering analysis of quasi-stellar objects (QSOs) as a function of luminosity over the redshift range $z = 0.3$ – 2.9 . We use a sample of 10 566 QSOs taken from the preliminary data release catalogue of the 2dF QSO Redshift Survey (2QZ). We analyse QSO clustering as a function of *apparent* magnitude. The strong luminosity evolution of QSOs means that this is approximately equivalent to analysing the data as a function of absolute magnitude relative to M^* over the redshift range that the 2QZ probes. Over the relatively narrow range in apparent magnitude of the 2QZ we find no significant ($>2\sigma$) variation in the strength of clustering, however, there is marginal evidence for QSOs with brighter apparent magnitudes having a stronger clustering amplitude. QSOs with $18.25 < b_J \leq 19.80$ show a correlation scalelength $s_0 = 5.50 \pm 0.79 h^{-1}$ Mpc in an Einstein–de Sitter (EdS) universe and $s_0 = 8.37 \pm 1.17 h^{-1}$ Mpc in a universe with $\Omega_0 = 0.3$ and $\lambda_0 = 0.7$ (Λ), while the best-fitting values for the full magnitude interval ($18.25 < b_J \leq 20.85$) over the same spatial scales are $s_0 = 4.29^{+0.30}_{-0.29} h^{-1}$ Mpc (EdS) and $s_0 = 6.35^{+0.45}_{-0.44} h^{-1}$ Mpc (Λ). We can therefore determine that the bias of the brightest subsample is a factor 1.22 ± 0.15 (EdS) or 1.24 ± 0.15 (Λ) larger than that of the full data set. An increase in clustering with luminosity, if confirmed, would be in qualitative agreement with models in which the luminosity of a QSO is correlated to the mass of the dark halo in which it resides, implying that the mass of the host plays at least some part in determining the formation of a QSO and evolution. These models predict that the clustering in brighter QSO data sets, such as the Sloan Digital Sky Survey QSO sample or the bright extension of the 2QZ, should show a higher clustering amplitude than the 2QZ.

Key words: galaxies: clusters: general – quasars: general – cosmology: observations – large-scale structure of Universe.

1 INTRODUCTION

The currently preferred models of structure formation based on hierarchical growth of structure predict that the level of clustering of a population is dependent on the mass of the dark halo in which the object resides. Thus clusters of galaxies should cluster much more strongly than galaxies do, which we observe to be the case. Analysis of galaxy surveys have also shown that more luminous (and therefore on average more massive) galaxies have stronger clustering than faint galaxies (Giavalisco & Dickinson 2001; Loveday et al. 1995).

The luminosity of quasi-stellar objects (QSOs) appears to be (weakly) correlated with host galaxy luminosity, at least for low-redshift QSOs (e.g. Schade, Boyle & Letawsky 2000). More luminous QSOs reside in brighter host galaxies. It is then natural to suppose that brighter QSOs should be found in more massive galaxies, assuming that luminosity and mass are correlated at least to some extent. Further circumstantial support for this argument is given by the correlation between the estimates of central black hole mass and the spheroidal component of the galaxies (Magorrian et al. 1998). We would then expect luminous QSOs to cluster more strongly than faint QSOs.

Until recently it was impossible to determine QSO clustering as a function of luminosity. The sparse nature of QSO surveys and the small numbers in homogeneous, complete samples meant that

*E-mail: scroom@aaopep.aao.gov.au

QSO clustering was only detectable at the $\sim 4\sigma$ level (Iovino & Shaver 1988; Andreani & Cristiani 1992; Shanks & Boyle 1994; Croom & Shanks 1996; La Franca, Andreani & Cristiani 1998). However, the 2dF QSO Redshift Survey (2QZ) has allowed a dramatic improvement to be made in the measurement of QSO clustering. Using over 10 000 QSOs from the 2QZ, Croom et al. (2001a) (henceforth Paper II) have made the first accurate (to ~ 10 per cent) measurement of QSO clustering. They find that QSO clustering averaged over the redshift range $0.3 \leq z \leq 2.9$ is very similar to that measured in redshift surveys of local ($z \sim 0.05$) galaxies. When fitting a standard power law of the form $\xi_Q(s) = (s/s_0)^{-\gamma}$ Croom et al. find $s_0 = 3.99^{+0.28}_{-0.34} h^{-1} \text{ Mpc}$ and $\gamma = 1.58^{+0.10}_{-0.09}$ for an Einstein–de Sitter Universe (henceforth denoted by EdS). For a cosmology with $\Omega_0 = 0.3$ and $\lambda_0 = 0.7$ (henceforth denoted by Λ) they find $s_0 = 5.69^{+0.42}_{-0.50} h^{-1} \text{ Mpc}$ and $\gamma = 1.56^{+0.10}_{-0.09}$. When investigated as a function of redshift the clustering of QSOs was found to be constant over the whole redshift range considered.

The nature of any flux-limited sample means that the most distant objects in the data set will on average have the highest intrinsic luminosity. There is then the reasonable concern that a comparison of QSO or galaxy clustering at different redshifts in any flux-limited sample is actually measuring the properties of a different population of objects at each redshift. In the case of QSOs, their extreme evolution in luminosity [$\propto (1+z)^3$] out to $z \sim 2$ (Boyle et al. 2000, henceforth Paper I) means that at each redshift we are at least studying the same part of the QSO luminosity function (LF).

In this paper we will make the first attempt to determine the strength of QSO clustering as a function of luminosity. In Section 2 we describe the data and analysis used. In Section 3 we present our clustering results from the 2QZ, these are discussed in Section 4.

2 DATA AND ANALYSIS

2.1 The QSO sample

For the analysis in this paper we have used the first public release catalogue of the 2QZ, the 10k catalogue (Croom et al. 2001b, henceforth Paper V). We only use QSOs with high-quality (quality Class 1; see Paper V) identifications of which there are 10 689 in the 10k catalogue (note that the number of QSOs used in the analysis of Paper II was 10 681, eight further QSOs were added to the 10k sample prior to its final publication). This 10k catalogue contains the most spectroscopically complete fields observed prior to 2000 November and is now publicly available to the astronomical community at <http://www.2dfquasar.org>. The sample contains 10 566 QSOs in the redshift range $0.3 < z \leq 2.9$, which will be included in our analysis below.

The magnitude range of the 2QZ is $18.25 < b_j \leq 20.85$. This is a fairly narrow range, covering just over an order of magnitude in flux. However, it does span the important regime in which the QSO luminosity function flattens towards fainter magnitudes. The distribution of QSO absolute magnitudes versus redshift is shown in Fig. 1 for the EdS cosmology. We convert from apparent to absolute luminosity using the k -correction of Cristiani & Vio (1990) and assume a Hubble constant of $H_0 = 50 \text{ km s}^{-1} \text{ Mpc}^{-1}$ (for luminosity determinations only). We note that in our clustering analysis we include the factor h where $H_0 = 100h^{-1} \text{ km s}^{-1} \text{ Mpc}^{-1}$. The objects at high redshift are on average much more luminous, as we would expect in a flux-limited sample. Also, as the number of QSOs drops dramatically at brighter apparent luminosities there is only a small amount of overlap in intrinsic luminosity between QSO samples selected at widely differing redshifts.

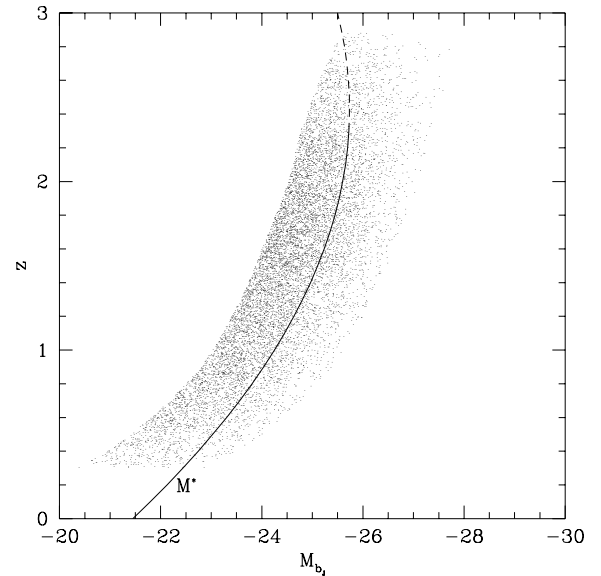


Figure 1. The redshift versus absolute magnitude distribution of 2QZ QSOs used in our analysis for an EdS cosmology. The solid line shows the value of M^* as a function of redshift, as derived from the best-fitting LF model (see text). The model fit is calculated between $z = 0.3$ and 2.3 , beyond $z = 2.3$ the model is an extrapolation (dashed line).

The QSO LF is well described by a double power law. The characteristic absolute magnitude of the break is denoted by M^* , which is found to evolve strongly with redshift. Using the power-law evolution model of Paper I, in which $M^*(z) = M^*(0) - 2.5(k_1 z + k_2 z^2)$, Paper V derived the best-fitting parameters for the 2QZ 10k catalogue and Large Bright Quasar Survey (Hewett, Foltz & Chaffee 1995) combined in an EdS universe. The parameters found were $\Phi^* = 0.2 \times 10^{-5} \text{ Mpc}^{-3} \text{ mag}^{-1}$, $\alpha = 3.28$, $\beta = 1.08$, $M_b^* = -21.45$, $k_1 = 1.41$ and $k_2 = -0.29$. M^* as a function of redshift for this model is plotted in Fig. 1. The fit to the LF is only carried out below $z = 2.3$, above that redshift the dashed line shows the extrapolation of the best-fitting model, which is approximately consistent with the density of high-redshift QSOs ($3.6 \leq z \leq 5$) found in the Sloan Digital Sky Survey (Fan et al. 2001). We have also fitted the same model to the 2QZ and LBQS assuming a Λ cosmology. In this case we find: $\Phi^* = 0.46 \times 10^{-6} \text{ Mpc}^{-3} \text{ mag}^{-1}$, $\alpha = 3.42$, $\beta = 1.35$, $M_b^* = -22.54$, $k_1 = 1.34$ and $k_2 = -0.26$. This fit is in the range of acceptability specified in Paper I ($P_{\text{KS}} > 0.01$) with a two-dimensional Kolmogorov–Smirnov (KS) probability of 0.02. It is worth noting that the parameters of these fits are strongly correlated, hence the use of any single parameter is to be discouraged. As this is the case we make comparisons between QSO samples of different *apparent* magnitudes, and do not split the QSOs in luminosity relative to M^* .

The division of QSOs on the basis of their apparent magnitude has several advantages over using absolute luminosities. First, apparent magnitude is a measured, not derived, quantity and is thus not dependent on the cosmological model used. It should be easy to produce flux-limited samples from any model of QSO formation, allowing direct comparison between data and models. Secondly, because M^* is at approximately the same apparent magnitude at every redshift, an apparent magnitude cut selects the same part of the QSO LF at each redshift.

Measuring the clustering of QSOs as a function of luminosity is challenging. In particular, at luminosities brighter than M^* the

Table 1. 2QZ clustering results as a function of limiting apparent magnitude. The fits assume a fixed power-law slope equal to that of the best fit from the full data set. The listed χ^2 value is a reduced χ^2 for the best fit.

(Ω_0, λ_0)	b_J range	\bar{b}_J	\bar{z}	\bar{M}_b	N_Q	s_0	χ^2	$\bar{\xi}(20)$
(1.0, 0.0)	$18.25 < b_J \leq 19.80$	19.29	1.398	-25.05	3518	$5.50^{+0.79}_{-0.79}$	1.70	0.236 ± 0.077
(1.0, 0.0)	$19.80 < b_J \leq 20.40$	20.12	1.509	-24.43	3697	$2.83^{+1.04}_{-1.24}$	0.93	0.171 ± 0.072
(1.0, 0.0)	$20.40 < b_J \leq 20.85$	20.63	1.552	-23.98	3351	$4.01^{+0.95}_{-0.98}$	0.34	0.206 ± 0.082
(0.3, 0.7)	$18.25 < b_J \leq 19.80$	19.29	1.398	-25.70	3518	$8.37^{+1.17}_{-1.17}$	0.75	0.722 ± 0.152
(0.3, 0.7)	$19.80 < b_J \leq 20.40$	20.12	1.509	-25.11	3697	$4.05^{+1.59}_{-1.90}$	0.76	0.317 ± 0.132
(0.3, 0.7)	$20.40 < b_J \leq 20.85$	20.63	1.552	-24.67	3351	$5.92^{+1.45}_{-1.49}$	0.83	0.358 ± 0.150

number density of QSOs falls off as a steep power law. Splitting a sample into N redshift bins of equal numbers of QSOs increases the error on pair counts by $\sim\sqrt{N}$. Dividing the sample into N luminosity bins increases errors by $\sim N\sqrt{N}$, as the surface density of sources is also reduced. This is a further reason why we limit our analysis in this paper to clustering as a function of apparent magnitude, as to carry out a meaningful subdivision on the basis of absolute magnitude requires a larger number of bins (owing to the redshift–luminosity degeneracy inherent in the data set). A method to reduce the error in the measured clustering as a function of absolute luminosity is to cross-correlate QSOs of a particular luminosity with all other QSOs. This method will be investigated by Loaring et al. (in preparation).

2.2 Correlation function estimates

Our correlation function estimation is carried out as described in Paper II. For completeness we outline the procedure here. The QSO correlation function, $\xi_Q(s)$, where s is the redshift-space separation of two QSOs, is calculated using two representative cosmologies, the EdS and Λ models. The minimum variance estimator of Landy & Szalay (1993) is used to derive $\xi_Q(s)$. In this paper we divide the 2QZ 10k sample into three apparent magnitude intervals with approximately equal numbers of QSOs. The magnitude ranges, mean redshifts and other parameters for these bins are listed in Table 1. We note that the mean redshifts of the different magnitude slices are very similar, with $\bar{z} = 1.398$, 1.509 and 1.552 for the bright, middle and faint slices, respectively. These small differences cannot introduce a significant variation in clustering, particularly as we find that QSO clustering does not evolve significantly with redshift (Paper II). The redshift distributions are shown in Fig. 2.

We correct for the current incomplete observational coverage of the survey by using a random catalogue that exactly traces the distribution of observed QSOs on the sky, as in Paper II. The redshift distribution of these random points is taken from a spline fit to the QSO $n(z)$ distribution (each magnitude slice is fitted separately). We also normalize the number of randoms within each UKST field in the survey to remove any possible systematic errors owing to zero-point calibration errors.

We calculate the errors on ξ_Q using the Poisson estimate of

$$\Delta\xi_Q(s) = \frac{1 + \xi(s)}{\sqrt{QQ(s)}}. \quad (1)$$

At small scales, $\lesssim 50h^{-1}$ Mpc, this estimate is accurate because each QSO pair is independent (i.e. the QSOs are not generally part of another pair at scales smaller than this). On scales larger than $\sim 50h^{-1}$ Mpc the QSO pairs become more correlated and we use the approximation that $\Delta\xi_Q(s) = [1 + \xi_Q(s)]/\sqrt{N_Q}$, where N_Q is the total number of QSOs used in the analysis (Shanks & Boyle

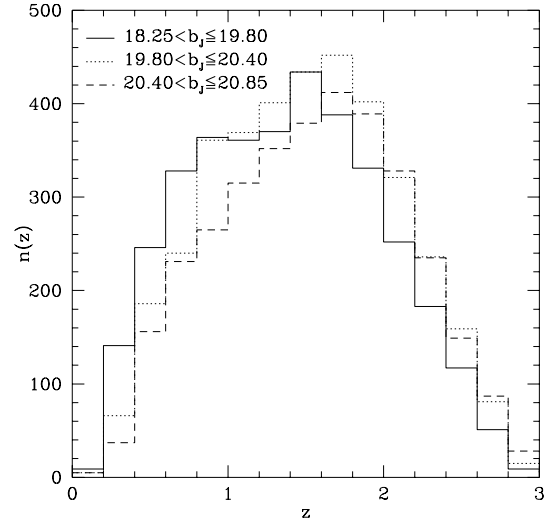


Figure 2. The QSO redshift distribution for our three apparent magnitude intervals, $18.25 < b_J \leq 19.80$ (solid line), $19.80 < b_J \leq 20.40$ (dotted line) and $20.40 < b_J \leq 20.85$ (dashed line).

1994; Croom & Shanks 1996), for bins in which $QQ(s) > N_Q$. Note that in this paper we are concerned with analysis on small scales ($\lesssim 25h^{-1}$ Mpc), where the Poisson error estimates are applicable. The $\sqrt{N_Q}$ errors are only used for displaying our correlation functions. On very small scales the number of QSO–QSO pairs can be $\lesssim 10$. In this case simple *root-n* errors (equation 1) do not give the correct upper and lower confidence limits for a Poisson distribution. We use the formulae of Gehrels (1986) to estimate the Poisson confidence intervals for one-sided 84 per cent upper and lower bounds (corresponding to 1σ for Gaussian statistics). These errors are applied to our data for $QQ(s) < 20$. By this point *root-n* errors adequately describe the Poisson distribution.

3 QSO CLUSTERING AS A FUNCTION OF LUMINOSITY

In Fig. 3 we show the clustering of 2QZ QSOs for three different apparent magnitude intervals (see Table 1) in an EdS universe. The best fit to the total sample found in Paper II is shown as the dotted line for reference. On scales $< 20h^{-1}$ Mpc it appears that the brighter QSOs (Fig. 3a) show marginally higher clustering than fainter QSOs (Figs 3b and c). In order to determine the significance of this difference we make two measurements. We first determine the integrated correlation function, $\bar{\xi}_Q$, within a radius s_{\max} , which is defined as

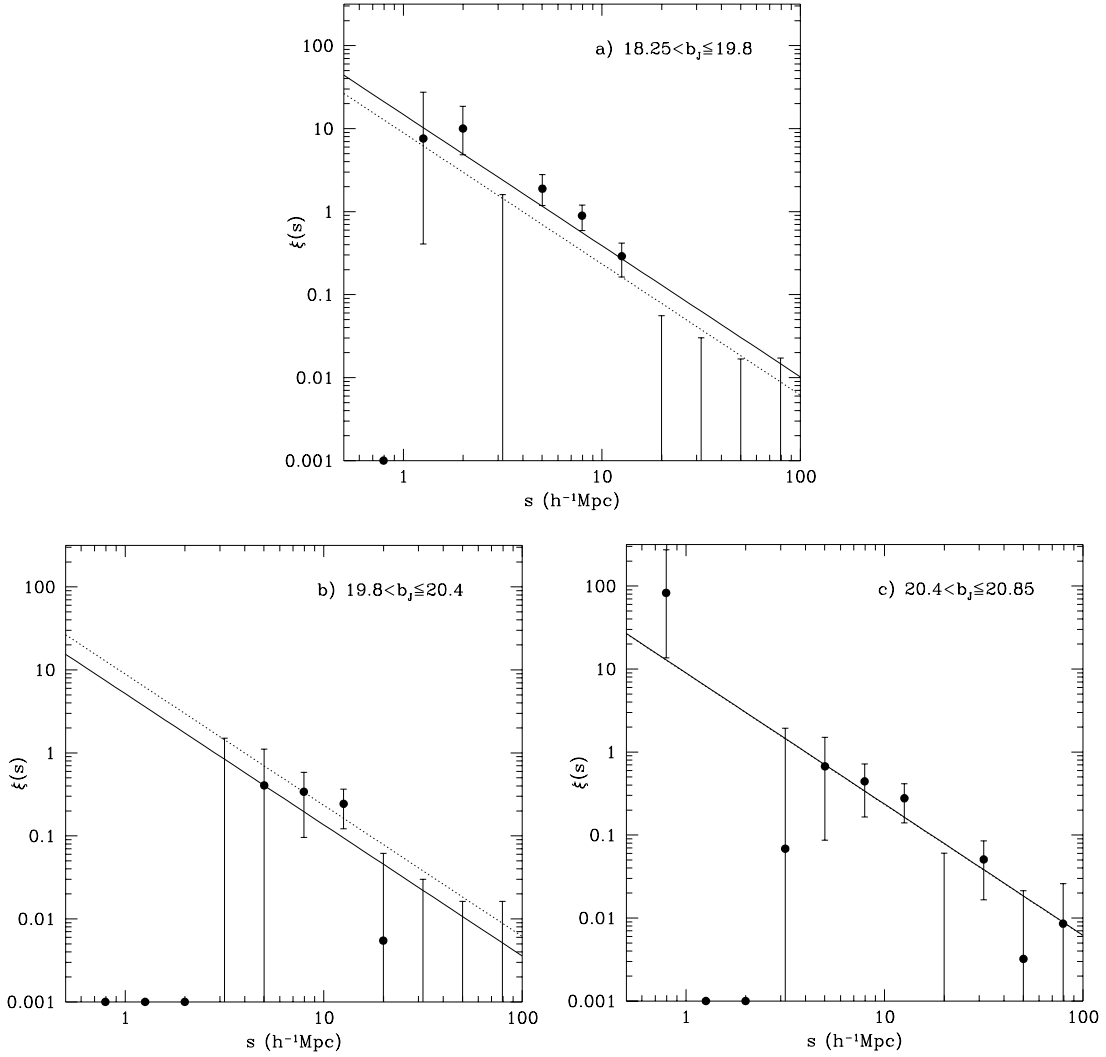


Figure 3. The clustering of QSOs as a function of limiting apparent magnitude in an EdS universe: (a) bright QSOs with $18.25 < b_J \leq 19.8$, (b) intermediate QSOs with $19.8 < b_J \leq 20.4$ and (c) faint QSOs with $20.4 < b_J \leq 20.85$. The solid line is the best-fitting power law in each case (assuming a slope of -1.58). The dashed line is shown for reference and is the best-fitting power law for the full sample from Paper II. The points at $\xi(s) = 0.001$ with no errors denote bins where no QSO–QSO pairs were found. These are properly taken into account in the fitting process.

$$\bar{\xi}_Q(s_{\max}) = \frac{3}{s_{\max}^3} \int_0^{s_{\max}} \xi_Q(x) x^2 dx. \quad (2)$$

We use $s_{\max} = 20h^{-1}$ Mpc as in Paper II. The results of this are shown in Table 1. While $\bar{\xi}_Q(20)$ is greatest for the bright sample, it is not significantly larger than the values found for fainter QSOs.

While $\bar{\xi}_Q$ is a robust statistic, it does not take into account the shape of ξ_Q . It is possible that a stronger constraint may be obtainable by fitting a functional form to the data. We fit a standard power law of the form $\xi_Q(s) = (s/s_0)^{-\gamma}$ to our results. We make the assumption that the slope of the power law does not vary with luminosity and fix the slope of the power law, to be the best fit from the full data set, that is, $\gamma = 1.58$ (EdS) or $\gamma = 1.56$ (Λ). We use a maximum-likelihood estimator based on the Poisson probability distribution function, so that

$$L = \prod_{i=1}^N \frac{e^{-\mu} \mu^{\nu}}{\nu!} \quad (3)$$

is the likelihood, where ν is the observed number of QSO–QSO pairs, μ is the expectation value for a given model and N is the number of bins fitted. We fit the data with bins $\Delta \log(r) = 0.1$, although we note that varying the bin size by a factor of 2 makes no noticeable difference to the resultant fit. In practice we minimize the function $S = -2 \ln(L)$, and determine the errors from the distribution of ΔS , where ΔS is assumed to be distributed as χ^2 . This procedure does not give us an absolute measurement of the goodness-of-fit for a particular model. We therefore also derive a value of χ^2 for each model fit in order to confirm that it is a reasonable description of the data. We carry out the fit on scales $0.7 < s \leq 20h^{-1}$ Mpc, the scales chosen being the smallest scale containing a QSO–QSO pair and the scale at which ξ_Q appears to break from a power law.

The best-fitting models are shown in Fig. 3 (solid lines). As suggested by the $\bar{\xi}_Q$ measurements, the brightest sample does show stronger clustering than the other samples, however the difference is only marginally significant. It should also be noted that the lowest clustering amplitude is found in the intermediate sample, although the fit to this data set is consistent with that of the faintest sample.

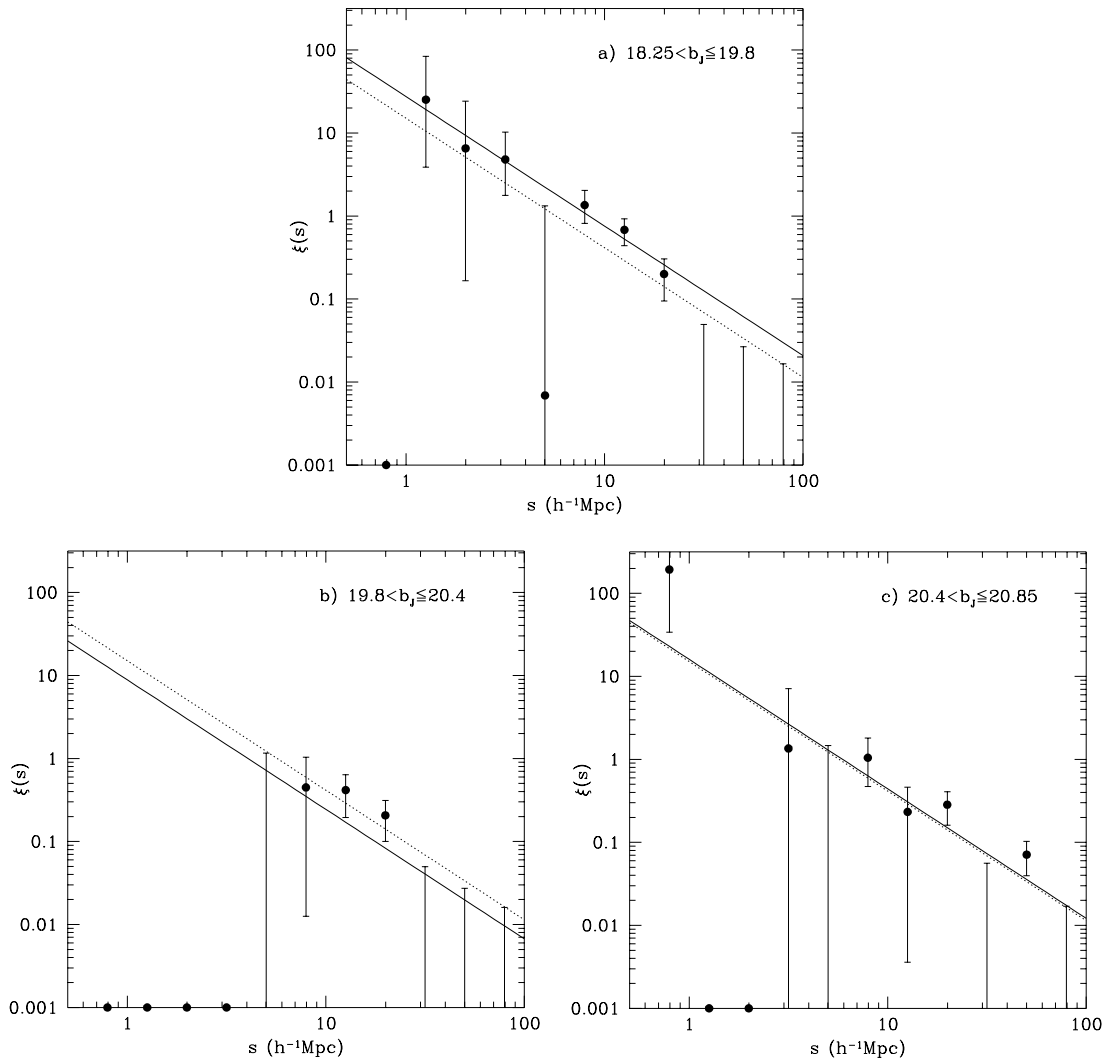


Figure 4. The clustering of QSOs as a function of limiting apparent magnitude in a Λ universe: (a) bright QSOs with $18.25 < b_J \leq 19.8$, (b) intermediate QSOs with $19.8 < b_J \leq 20.4$ and (c) faint QSOs with $20.4 < b_J \leq 20.85$. The solid line is the best-fitting power law in each case (assuming a slope of -1.56). The dashed line is shown for reference and is the best-fitting power law for the full sample from Paper II.

In Fig. 4 we plot the clustering of QSOs in a Λ universe. This shows the same feature as the EdS case, with the brightest QSOs being the most strongly clustered. The measured $\xi_Q(20)$ values (Table 1) also show this. The significance of the difference between the faintest and brightest subsamples is now larger, but still only at the $\sim 1.7\sigma$ level. We carry out the power-law fit (this time between $0.8 < s \leq 25 h^{-1}$ Mpc) as above (solid lines), again finding only a marginal difference between different magnitude intervals.

In Fig. 5 we plot the fitted values of s_0 as a function of mean apparent magnitude. In order to show a convincing trend as a function of magnitude we would like to span a much larger range in magnitude than is possible with the current sample.

4 DISCUSSION

Fitting the full data set over the same range of scales as above we find that $s_0 = 4.29^{+0.30}_{-0.29} h^{-1}$ Mpc (EdS) and $s_0 = 6.351^{+0.45}_{-0.44} h^{-1}$ Mpc (Λ). Thus the brightest third of QSOs has a clustering scalelength, which is a factor of 1.28 ± 0.20 (EdS) or 1.32 ± 0.20 (Λ) larger than that of the full sample. As $b/b^* = (s_0/s_0^*)^{1/2}$ this then implies that

the ratio of the biases is 1.22 ± 0.15 (EdS) or 1.24 ± 0.15 (Λ). We therefore find only weak evidence that bright QSOs cluster more strongly.

We should also consider comparing the above results with other measurements of luminosity dependent clustering. The most accurate measurement of this to date is by Norberg et al. (2001) using data from the 2dF Galaxy Redshift Survey. Norberg et al. find that the clustering of $z < 0.3$ galaxies is a weak function of luminosity fainter than L_g^* , but a much stronger function of luminosity for galaxies brighter than L_g^* . They find that the relation $b_g/b_g^* = 0.85 + 0.15 L_g/L_g^*$ well describes the luminosity dependence of galaxy bias, b_g , relative to that found for L_g^* galaxies. If there was a simple one-to-one relation between galaxy luminosity and QSO luminosity, we would be able to make a straightforward comparison of QSO clustering with this relation. Unfortunately, we know that there is only a weak correlation (with large dispersion) between these two quantities (Schade et al. 2000). We can, however, at least check for consistency between the galaxy and QSO clustering luminosity dependence. Under the assumption that galaxy luminosity is more closely related to halo mass than QSO luminosity is, we would

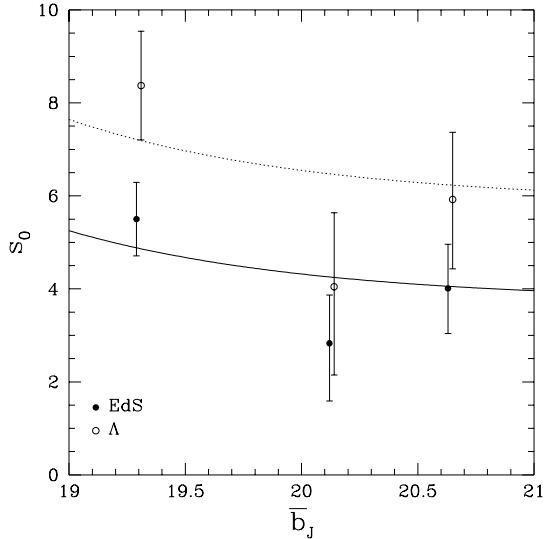


Figure 5. The QSO clustering scalelength, s_0 as a function of mean apparent magnitude in an EdS universe (filled circles) and a Λ universe (open circles). The best-fitting galaxy luminosity dependence models (see Section 4) for EdS (solid line) and Λ (dotted line) cosmologies are also shown.

expect the change in QSO clustering with luminosity to be no more rapid than the change in galaxy clustering with luminosity. Converting the above relation for galaxy clustering into a form directly applicable in our case we find $(s_0/s_0^*)^{1/2} = 0.85 + 0.15 \times 10^{-0.4(m-m^*)}$, where m^* is the apparent magnitude corresponding to M^* . The value of m^* varies in the range 19.3–19.6 depending on the particular best-fitting LF model used. We assume throughout that b is not a function of scale and allow s_0^* to be a single free parameter, while fixing m^* [$m^* = 19.6$ (EdS) or 19.3 (Λ)]. The best-fitting values are $s_0^* = 4.78 \pm 0.57h^{-1}$ Mpc (EdS) or $s_0^* = 7.20 \pm 0.86h^{-1}$ Mpc (Λ) and lines corresponding to these are shown in Fig. 5. We find that the above empirical model for galaxies is also consistent with the clustering of QSOs in the 2QZ. However, this is unsurprising given the large errors on the QSO clustering measurements.

A number of authors have attempted to model the clustering of QSOs, based on the formalism of Press & Schechter (1974) for describing the evolution of dark matter haloes (Martini & Weinberg 2001; Haiman & Hui 2001). These make the assumption that the luminosity of QSOs is correlated with the mass of the dark matter halo in which they reside. Although there is reasonable evidence that the *mass* of compact objects (presumably black holes) is correlated with the mass of the spheroidal component of the host galaxy (e.g. Magorrian et al. 1998), a correlation between AGN *luminosity* and host luminosity and/or mass is less evident. The time-scale of QSO activity is the main parameter that controls the amplitude of clustering in these models, with time-scales of the order

of 10^6 yr being most consistent with the results found in Paper II (Kauffmann & Haehnelt 2002). The main arguments are based on the number-density of galaxies that have gone through a QSO phase. Similar number-density arguments suggest that, as brighter QSOs are rarer, they should cluster more strongly. Our current analysis does not have sufficient signal-to-noise ratio to clearly demonstrate this, and a more detailed investigation will have to await brighter QSO surveys such as the Sloan Digital Sky Survey (Schneider et al. 2002) and the bright extension to the 2QZ being carried out with FLAIR and the 6 degree field system on the UK Schmidt Telescope. Further investigation is also possible using other techniques, such as the *cross-correlation* of QSOs of different luminosities. This will be investigated in the 2QZ by Loaring et al. (in preparation).

ACKNOWLEDGMENTS

We warmly thank all the present and former staff of the Anglo-Australian Observatory for their work in building and operating the 2dF facility. The 2QZ is based on observations made with the Anglo-Australian Telescope and the UK Schmidt Telescope. NSL is supported by a PPARC Studentship.

REFERENCES

- Andreani P., Cristiani S., 1992, *ApJ*, 398, L13
 Boyle B. J., Shanks T., Croom S. M., Smith R. J., Miller L., Loaring N., Heymans C., 2000, *MNRAS*, 317, 1014 (Paper I)
 Cristiani S., Vio R., 1990, *A&A*, 227, 385
 Croom S. M., Shanks T., 1996, *MNRAS*, 281, 893
 Croom S. M., Shanks T., Boyle B. J., Smith R. J., Miller L., Loaring N., Hoyle F., 2001a, *MNRAS*, 325, 483 (Paper II)
 Croom S. M., Smith R. J., Boyle B. J., Shanks T., Loaring N. S., Miller L., Lewis I. J., 2001b, *MNRAS*, 322, L29 (Paper V)
 Fan X. et al., 2001, *AJ*, 121, 54
 Gehrels N., 1986, *ApJ*, 303, 336
 Giavalisco M., Dickinson M., 2001, *ApJ*, 550, 177
 Haiman Z., Hui L., 2001, *ApJ*, 547, 27
 Hewett P. C., Foltz C. B., Chaffee F. H., 1995, *AJ*, 109, 1499
 Iovino A., Shaver P. A., 1988, *ApJ*, 330, L13
 Kauffmann G., Haehnelt M., 2002, *MNRAS*, 332, 529
 La Franca F., Andreani P., Cristiani S., 1998, *ApJ*, 497, 529
 Landy S. D., Szalay A. S., 1993, *ApJ*, 412, 64
 Loveday J., Maddox S. J., Efstathiou G., Peterson B. A., 1995, *ApJ*, 442, 457
 Magorrian J. et al., 1998, *AJ*, 115, 2285
 Martini P., Weinberg D. H., 2001, *ApJ*, 547, 12
 Norberg P. et al., 2001, *MNRAS*, 328, 64
 Press W. H., Schechter P., 1974, *ApJ*, 187, 425
 Schade D. J., Boyle B. J., Letawsky M., 2000, *MNRAS*, 315, 498
 Schneider D. P. et al., 2002, *AJ*, 123, 567
 Shanks T., Boyle B. J., 1994, *MNRAS*, 271, 753

This paper has been typeset from a $\text{\TeX}/\text{\LaTeX}$ file prepared by the author.